

## ABSTRACT

Title of Document: SOLVENT STUDY ON MICRO TOWERS  
FABRICATED VIA MAP

Yunbo Shi, Master of Science, 2008

Directed By: Professor John T. Fourkas  
Department of Chemistry and Biochemistry

Common microfabrication techniques have been briefly reviewed and a detailed description of multiphoton absorption polymerization (MAP) ranging from its history, specific experimental setup, and resolution to its applications and drawbacks has also been given. A fast method to fabricate micro towers via MAP has been found. Towers with diameters ranging from 900 nm to 6 microns were fabricated and the best aspect ratio ( $\sim 40$ ) does not change with the diameter of the towers. Different solvents were used to dry those towers and we found that surface tension is not the only factor that leads to lower aspect-ratio.

SOLVENT STUDY ON MICRO TOWERS FABRICATED VIA MAP

By

Yunbo Shi

Thesis submitted to the Faculty of the Graduate School of the  
University of Maryland, College Park, in partial fulfillment  
of the requirements for the degree of  
Master of Science  
2008

Advisory Committee:  
Professor John T. Fourkas, Chair  
Professor Amy Mullin  
Professor Michael Zachariah

© Copyright by  
Yunbo Shi  
2008

## Acknowledgements

I would like to thank my parents and my elder sister first because they support every decision I make. Without their life-long support and encouragement, I could not have walked this far, nor would I be able to continue to strive for success.

I would also like to express my deep and sincere gratitude to my supervisor, John Fourkas. Dr Fourkas is the smartest guy I have ever worked with and I am really honored to work under his guidance. Many of his ideas are very inspirational and they always work, I mean, in most cases. I would recommend him to any new graduate students who really have passion for science. I really appreciate his understanding and support when I told him I had to leave this group, which brought me enjoyable and memorable experiences in the past two years.

I consider myself very fortunate to know Kathleen Monaco when we joined the group at the same time. We always encouraged each other and helped each other in our life and work.

I am grateful to Linjie Li and Qin Zhong, who helped me a lot when I came to the United States two years ago. They also taught me a lot to get me started with the operations in the lab.

I wish to thank Dr George Kumi for proofreading my thesis carefully and patiently. I would also like to thank Meghan Driscoll for the delightful physics discussions we made together and Mike Stocker for his practical jokes.

Finally, I would like to acknowledge other members in Fourkas' group that I have the pleasure to work with: Soner Erduran, Hana Hwang, Terry Ding, Sanghee Nah and Rafael Gattass. They all have been great colleagues and friends.

# Table of Contents

List of Tables	v
List of Figures	vi
Chapter 1: Introduction to Microfabrication Techniques .....	1
1.1 Introduction to Microfabrication.....	1
1.2 Common Microfabrication Techniques .....	1
1.3 Thesis Outline .....	3
Chapter 2: Multiphoton Absorption Polymerization .....	5
2.1 Multiphoton Absorption.....	5
2.2 Multiphoton Absorption Polymerization .....	6
2.2.1 Experimental Setup.....	6
2.2.2 Materials .....	7
2.2.3 Photoinitiators .....	10
2.2.4 Resolutions.....	12
2.2.5 Applications .....	13
2.2.6 Drawbacks.....	15
Chapter 3: Solvent Study on Towers Fabricated via MAP .....	19
3.1 Introduction.....	19
3.2 Experimental Details.....	20
3.3 Results and Discussions .....	22
3.3.1 Methods.....	22
3.3.2 Size Study .....	23
3.3.3 Solvent Study .....	25
3.3.4 Applications .....	27
3.4 Summary .....	28
Chapter 4: Conclusion.....	30
References.....	31

## List of Tables

Table 1 Critical heights for towers with different diameters

## List of Figures

Figure 1 One photon fluorescence and two photon fluorescence	5
Figure 2 Experimental setup for MAP	7
Figure 3 Molecular Structure of Lucirin TPOL	12
Figure 4 Schematic illustration of the mechanism of the pattern distortion	17
Figure 5 Towers fabricated via three methods	23
Figure 6 Proof of existence of critical height	23
Figure 7 H-D graph for microtowers fabricated via MAP	25
Figure 8 Dependence of critical height on the drying solvent	26
Figure 9 Fast microfabrication of towers and pipes	28

# Chapter 1: Introduction to Microfabrication Techniques

## 1.1 Introduction to Microfabrication

Microfabrication techniques have brought great changes to this world, and in particular these methods have made immense contributions to the development of the electronics industry. Small integrated circuits and micro transistors are fabricated and widely used in various portable electronic devices such as computers. For example, Intel has recently made a brand new Itanium quad-core Central Processing Unit (CPU) with a record-busting two billion transistors and with individual feature sizes reaching 45 nanometers (from [www.intel.com](http://www.intel.com)). Furthermore, microfabrication is also essential for other emerging areas such as microelectromechanical systems (MEMS), micro-total analysis system<sup>1</sup> and microfluidics,<sup>2</sup> etc.

## 1.2 Common Fabrication Techniques

Of the numerous micro patterning methods, photolithography is the process most widely used. Photolithography uses light to transfer a geometric pattern from a photomask to a light-sensitive chemical, called a photoresist, on the substrate (usually a silicon wafer). It is a powerful technique due to its high resolution and its ability to fabricate thousands of patterns in parallel. However, it also suffers from several problems that prevent it from being used in MEMS and other chemical or biological systems. Firstly, a clean room is always required, which is beyond the reach of many researchers. Secondly, the materials that can be used as photoresists are quite limited. Finally, it is essentially a 2D fabrication technique. While different layers can be

stacked together to form 3D structures, complex 3D structures cannot be made simply with photolithography.

Other advanced lithographic techniques developed as potential substitutes for conventional photolithography include X-Ray lithography<sup>3</sup> and electron beam lithography, which can generate very small features with high resolution (nm scale). The structures fabricated by these procedures have smooth surfaces. However, their development into economical methods for mass-production still requires substantial effort and they can only produce limited 3D features.

Soft lithography<sup>4</sup> is another popular alternative. It uses photolithography or electron beam lithography to generate patterns that are molded by elastomers, typically polydimethylsiloxane (PDMS), to create a stamp. The stamp can then be used to duplicate structures with nanometer resolution using a wide variety of materials, which cannot be achieved by photolithography. Whitesides and coworkers<sup>4</sup> have demonstrated many applications of this technique in various fields such as materials science, optics, MEMS, and microelectronics. Soft lithography is cheap and convenient, but it can only be used to fabricate restricted 3D structures because it starts with photolithography or electron lithography.

To create arbitrary 3D structures other commonly used techniques such as self-assembly and microstereolithography<sup>5,6</sup> ( $\mu$ SL) are employed. While self-assembly is commonly seen in biological systems, it is not easy to control in the laboratory.  $\mu$ SL utilizes focused light to scan over the surface of a photo-curable resin, which undergoes photo-polymerization and forms solid microstructures. Once one layer is built, another layer of fresh resin needs to be flowed and the process is repeated.

While  $\mu$ SL can be used to produce highly precise, three-dimensional (3D) complex microstructures from broad selection of functional materials, it is generally a slow process because the flow process needs high precision and takes a long time due to the high viscosity of resin<sup>6</sup>.

However, multi-photon absorption polymerization (MAP) [also known as two-photon absorption polymerization (TPP)] allows for the patterning of photo-active materials with true 3D spatial resolution and provides a method for the direct laser writing of arbitrary 3D structures. MAP has developed significantly since its inception due to its low cost and ability to fabricate complex 3D features with high resolution. I will specifically talk about it in the following chapter.

### 1.3 Thesis Outline

In this chapter, many common microfabrication techniques are briefly introduced and compared. In the second chapter, a detailed description of MAP ranging from its history, specific experimental setup, and resolution to its applications and drawbacks is given. Compared to conventional microfabrication techniques, MAP has been demonstrated to be a powerful technique to fabricate arbitrary 3D microstructures with sub-micron features and it might find great use in industry once some of its drawbacks are overcome.

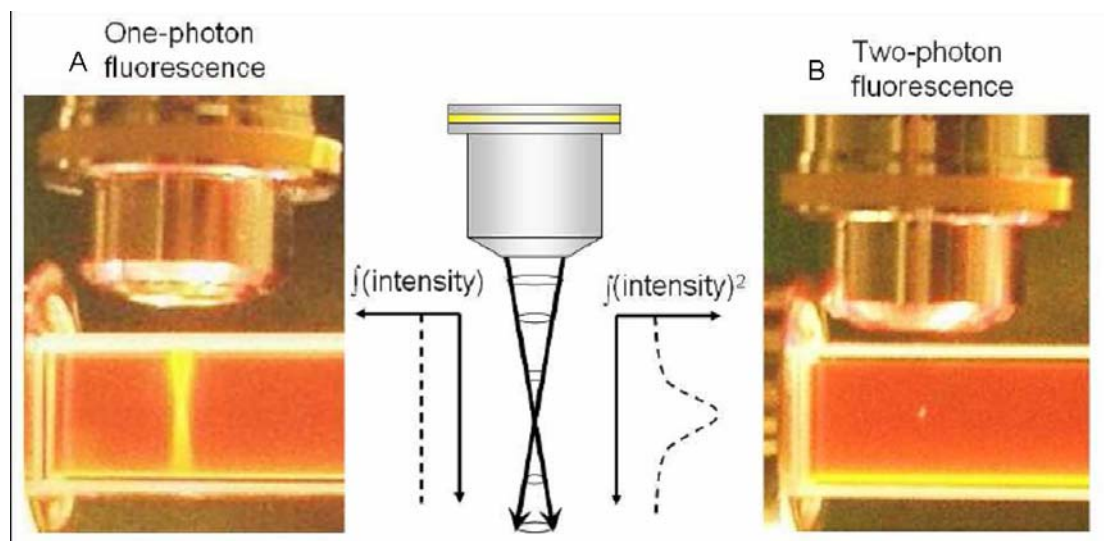
In the third chapter, micro towers will be fabricated via MAP in three ways and one of the methods will be chosen for the following two studies. The first study is size study, in which towers of different diameters are fabricated and the relationship between the best aspect ratio and the diameter of the micro towers is given. The

second one is to study the influence of the drying solvent on the best aspect ratio of towers with the same diameter. A rule to pick the best drying solvent for MAP is proposed and the best method to fabricate towers is then directly applied to the fabrication of standing pipes.

## Chapter 2: Multiphoton Absorption Polymerization

### 2.1 Multiphoton absorption

Two-photon absorption was first predicted by Maria Goeppert-Mayer in 1931<sup>7</sup> and in contrast to single photon absorption, two photons have to be absorbed simultaneously in TPA, which requires high intensities. Thus TPA could not be observed until the laser was invented in 1961. One of the most common applications of TPA is two-photon confocal microscopy<sup>8</sup>, where the fluorescence of a dye molecule is observed after being excited by means of TPA. Figure 1A) shows a single-photon excited fluorescence and you can see that light is scattered along the path; Figure 1B) shows fluorescence excited by TPA and the fluorescence is confined to the focal point.<sup>9</sup>



**Figure<sup>9</sup>** 1 A) Fluorescence in Rhodamine B caused by one photon excitation from a UV lamp. B) Fluorescence in Rhodamine B caused by two-photon excitation from a mode-locked Ti:sapphire operating with a wavelength of 800 nm.

In multi-photon absorption, two or more photons are involved in the excitation processes. One of the most important applications of multi-photon absorption is multi-photon absorption polymerization. (MAP).

## 2.2 Multiphoton Absorption Polymerization

The probability of multi-photon absorption by the photoinitiators is proportional to  $I^n$ , where  $I$  is the laser pulse energy and  $n$  is the number of photons involved in the process<sup>10</sup>. For two photon polymerization, the photo initiators absorption depends on the square of the laser intensity. Because of this nonlinear dependence on intensity, it is only possible to excite photo initiators within a focal volume of a laser beam that has been tightly focused by a microscope objective. Thus, the polymerization is only initiated within that small volume on the order of  $\lambda^3$ , where  $\lambda$  is the laser wavelength<sup>11</sup>. By scanning the focal point along the x, y, and z directions in a mixture of initiators and polymer monomers, desired 3D patterns with sub-micron size features can be fabricated.

### 2.2.1 Experimental Setup

A typical MAP system includes a pulsed laser and a strongly focusing lens, e.g. a high-numerical-aperture (NA) objective, which are used to generate the photo density necessary to initiate multi-photon absorption. Our system also includes optics for power control and steering, a commercial objective with CCD camera for viewing the process in real time, and a computer controlled 3-axis piezo stage for pattern generation. A 800 nm Ti:Sapphire laser is focused tightly and directed into a photoactive prepolymer resin through a high NA objective lens, and laser radiation is

used to excite the photon initiators to produce radicals or cations, which triggers polymerization within the focal volume. By moving the stage supporting the sample with respect to the focal point, 3-D structures of arbitrary geometry with submicrometer feature sizes can be fabricated<sup>12, 13, 14, 15</sup>. After the fabrication is complete, the unpolymerized resin is washed away using ethanol or another developer solvent and then the polymeric structure is dried in a different solvent.

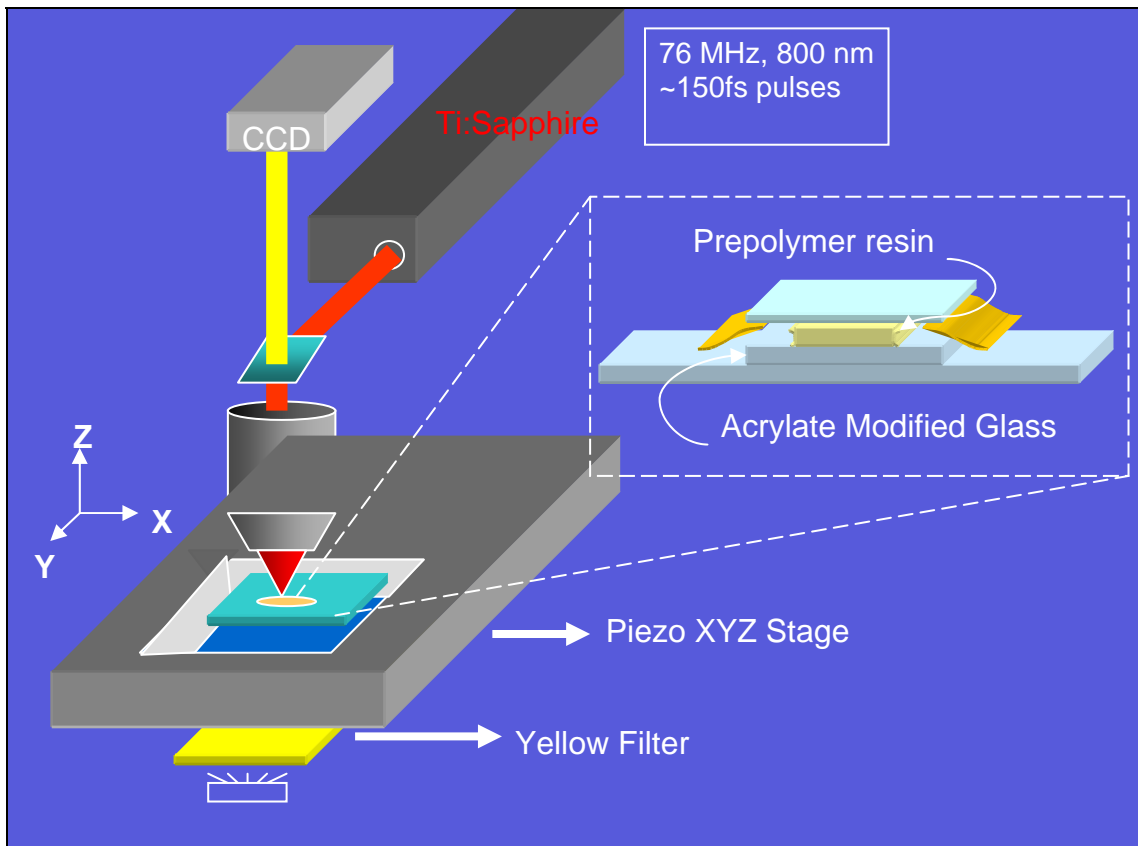


**Figure 2.** Diagram for experimental set-up of MAP.

### 2.2.2 Materials

Polymer materials are chosen for MAP because polymers are inexpensive and easy to process. Polymer materials are also flexible enough to be modified into composites to achieve chemical and physical functionality. Resins used to fabricate micro structures consist of monomers or oligomers and appropriate photoinitiators,

and there are some requirements for such resins: 1) they must be transparent in the visible and NIR region to avoid the interference of single-photon absorption polymerization, 2) they should have a fast curing speed so that the polymerized area is limited only to the focal point, 3) the highly cross-linked material must have some resistance to the solvent used in the later washout process and they cannot swell or be deformed in that process, 4) the polymerized resin must have some mechanical, thermal stability, or other properties needed to sustain their shape.

Many resins have been developed for MAP, and the corresponding initiators are chosen based on polymerization mechanisms, either radical polymerization or cationic polymerization.

For radical polymerization, the materials most commonly used in MAP are acrylic resins due to their high polymerization rates, wide variety and commercial availability. Kawata and coworkers<sup>12, 13, 14</sup> have used a resin consisting of urethane acrylate monomers, urethane acrylate oligomers as well as photo initiators, which is commercially known as SCR-500. They have done a lot of fabrication using this kind of resin.

Photosensitive inorganic-organic hybrid polymers (ORMOCERs, developed at the Fraunhofer Institut für Silicatforschung) have also been used in MAP<sup>15</sup>. These silicate-based materials are usually prepared by sol-gel methods. Inorganic (-Si-O-Si-) backbones in silicones are functionalized with organic groups such as acrylates or epoxies. Such compounds can form a firm solid after photo polymerization and have great potential use in fabricating optical devices with special properties. Bhuian<sup>16</sup> et al have described the synthesis and performance of a Zr-based inorganic-organic hybrid

system, cross-linked by the two-photon induced process. That material was produced by sol-gel synthesis using a silicon alkoxide species that also possessed methacrylate functionality. Stabilized zirconium alkoxide precursors were added to the precursor solution in order to reduce drying times and impart enhanced mechanical stability to deposited films.

For cationic photo-polymerization, commercialized SU-8 provided by MicroChem is the most commonly used resin, and it was originally developed for the microelectronic industry. The product is supplied as a liquid consisting of an epoxy resin, a solvent and a photo-acid generator. The substrate can be coated using a conventional spinner with the film thickness being controlled by the spinning speed and the resin concentration. A sample of pure liquid resin without solvent can also be sandwiched into two cover slips with a thin spacer, which determines the thickness of the polymer film. Upon exposure to a light beam, a strong acid in the resin is generated first, and this causes the epoxy resin to form a network with a high cross-linking density when the resin is heated above a critical temperature provided in a post-exposure bake. The unexposed material is then removed with a solvent in the development process. Because it is a two-step procedure, the formation of microstructures cannot be monitored during fabrication and it requires additional processing steps, such as a pre-exposure bake and a post-exposure bake and. Tech and coworkers<sup>17, 18</sup> have fabricated ultrahigh-aspect ratio plastic pillars, planes, and cage structures using SU-8 with low numerical aperture optics.

Although commercial resins have good performance, the composition of resins is changeable. Customer-made resins may have some benefits when some devices need

special requirement. Our group<sup>15</sup> has previously developed the acrylate-based resins with favorable chemical and physical properties for MAP. Their resin formulation has three components. The first component, ethoxylated(6) trimethylolpropane triacrylate helps to reduce shrinkage upon polymerization. The second component tris(2-hydroxyethyl) isocyanurate triacrylate promotes hardness of the polymer. The final component is Lucirin TPO-L, which I will talk about later.

### 2.2.3 Photoinitiators

The photoinitiator is of critical importance in the photon polymerization process. In a single photon process, an initiator absorbs one UV photon, through a linear absorption process, and breaks into radicals or ions. There are many well-known applications for single photon polymerization (e.g., UV-photolithography or stereolithography) where a single UV photon is needed to initiate the polymerization process near the surface of a photosensitive resin. Depending on the concentration of photoinitiators in the resin, UV light is absorbed by the resin within the first few micrometers from the resin surface. For multi-photon polymerization, two or more near infrared (NIR) photons are absorbed simultaneously by the photoinitiator, and this process requires the high radiation intensities of lasers. Moreover, this absorption only happens in a focal point within the volume of the resin, making MAP a true 3D fabrication technique. This type of absorption leads to better resolution.

Good photoinitiators for MAP usually have two characteristics. Firstly, they must have a large absorption cross section. Low TPA cross-sections mean low two-photon sensitivity<sup>14</sup>. Thus, high excitation power and long exposure time are needed to cure

the resin, which often results in damage to the structure. Secondly, they must be transparent in the near-infrared region of the spectrum to avoid the interference of single photon absorption polymerization. Many initiator systems have been developed for MAP, which makes the process more reliable and efficient.

Two types of photoinitiators are most commonly used in MAP. The first one is Norrish Type I radical initiators. Initiator cross-sections are usually improved by extending the conjugate system. Prasad et al.<sup>19, 20, 21</sup> have reported that one dimensional (1D) D- $\pi$ -A (Donor- $\pi$ -Acceptor) type molecules containing fluorine or dithienothiophene as the rigid p-conjugated backbone have large cross-sections. Marder et al.<sup>22, 23</sup> have demonstrated that the symmetric molecules with D- $\pi$ -A- $\pi$ -D and A- $\pi$ -D- $\pi$ -A structures are also characterized by large TPA cross sections. The other one is to optimize two component systems by changing coinitiators with known two-photon initiators (Type II). Belfield and coworkers<sup>24</sup> have demonstrated that N,N-dimethylaniline derivatives can act as highly efficient coinitiators for one-photon and two-photon photopolymerization of acrylates and methacrylates.

Although new photoinitiators with larger absorption cross-sections, a key factor for MAP, have been designed<sup>11,25</sup>, they are not readily available. We have demonstrated that Lucirin TPOL with a medium cross-section is an effective photoinitiator for MAP<sup>15</sup>. It is cheap and commercially available. In addition, it is a liquid with broad solubility and hence easily mixed with other resins. In the work described in this dissertation TPOL was always used as the photo initiator for MAP. Figure 3 is the molecular structure of Lucirin TPOL.

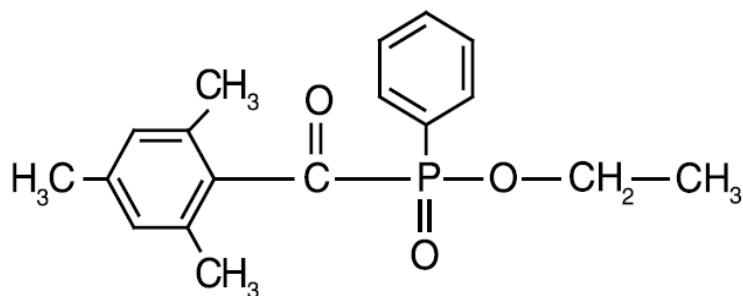


**Figure 3** Molecular Structure of Lucirin TPOL

### 2.2.4 Resolution

Resolution is one of the most important parameters for fabrication techniques. A number of years ago, a 120 nm lateral spatial resolution was achieved by Kawata. This was touted as a historical record of subdiffraction-limited laser fabrication, and it was attained via a radical quenching effect.<sup>12, 26</sup> Resolution is determined by the voxel size (the size of focal point), which involves three factors: absorbed photon number and spatial distribution (which are governed by exposure duration per voxel and NA, respectively), the concentration of the initiator, and the concentration of quencher. In our experiment, small voxel is achieved by reducing laser beam power, increasing the speed of the stage and using a higher NA objective.

Takada<sup>27</sup> et al have improved the spatial resolution from the previously reported value, 120 nm, to around 100 nm by intentionally introducing radical quenchers in the resin. They have also measured the roughness of the surfaces as 4 nm to 11 nm on a  $10\mu\text{m} \times 10\mu\text{m}$  area, which could fully satisfy the needs of photonic devices.

Haske and his coworkers<sup>28</sup> have reported a reliable fabrication of nanoscale polymeric features with widths as small as 65 nm using 520 nm femtosecond pulse

excitation of a 4,4'-bis(di-n-butylamino)biphenyl chromophore to initiate cross linking in a triacrylate blend. They have succeeded in applying this technique to fabricate polymeric woodpile photonic crystal structures that show stop bands in the near-IR spectral region.

The smallest feature so far is about 25 nm, which is achieved by Duan and coworkers<sup>29</sup>. They used femtosecond laser pulses at a wavelength of 780 nm and SCR-500 as the prepolymer resin. Lines with sub-25-nm width were produced by controlling the incident laser power and the laser focus scan speed. With the development of more effective photoinitiators and more advanced laser techniques, three-dimensional nanofabrication with high spatial resolution seems very promising in the future.

### 2.2.5 Applications

Quite a few applications have been reported in various fields such as photonics, MEMS, biology and microfluidics, etc. One application of MAP in photonics is the fabrication of photonic crystals. Photonic band-gap (PBG) materials have a three dimensional periodicity with a period in the range of the incident light wavelength. Because MAP is a 3D fabrication technique with resolution near 100 nm, many researchers have applied this technique in the fabrication of photonic crystals. Paul V. Braun and coworkers<sup>30</sup> have demonstrated the use of MAP to fabricate line and point defects in the interior of colloidal crystals and showed its great potential for defined defect fabrication within self-assembled photonic crystals for the development of PBG-based devices. Jesper Serbin and coworkers<sup>31</sup> have presented their results on the

construction of three dimensional photonic crystals by a two-photon-polymerization technique and the optical characterization of these crystals. They used two different classes of materials: Ormocers and SU-8, both of which show high transparency in the visible and near infrared ranges. Besides photonic crystals, photonic devices such as waveguides, splitters, and couplers for application in plasmonics have also been fabricated by this technique<sup>32,33</sup>.

In electronics, MAP has also been used to fabricate microelectronic devices, which may be an important component of MEMS. Mechanical structures with movable parts<sup>34</sup> or interlocking parts<sup>35</sup> have been fabricated. Most of the present work has focused on the functionalization and metallization of fabricated polymeric structures. Our group has used this method to fabricate functional microinductors on the 100 micron distance scale.<sup>36</sup> Metal is selectively deposited to the surface of the polymeric microinductors. The resonance frequencies of such inductors are in the GHz range, which is useful for communications devices, and can readily be lowered in the realm of MHz for applications in magnetic resonance. Those inductors are widely used in electronics as filters, transformers, and components of oscillator circuits. The metallization procedure shows great promise of the application of MAP in electronics.

In biological fields, MAP has demonstrated a great potential for many applications due to its 3D controllability and low cost. In the field of tissue engineering, which creates biocompatible and bioactive structures that are on the size scale of cells and tissues, biocompatible tissue scaffolds can be constructed to serve as active analogues of the extracellular matrix (ECM), where cells can attach,

proliferate, and ultimately synthesize their own matrix molecules. Campagnola<sup>37</sup> et al have introduced the use of multiphoton excited photo-crosslinking of proteins as a new 3D biofabrication method. They used this methodology to fabricate photo-crosslinked collagen (types I, II, and IV) structures on the sub-micrometer and micrometer size scales and have studied some of the resulting structural and functional aspects of these model scaffolds. The resulting structures display excellent retention of bioactivity as evidenced by highly specific cell adhesion as well as immunofluorescence labeling, which suggests that the multiphoton fabrication process may be a powerful tool for the creation of cell-sized tissue engineering scaffolds. In the field of microfluidics, which is dominated by soft lithography, MAP may allow for the direct fabrication of micro channels<sup>38</sup>. Besides, due to its ability to fabricate optical devices, it may also play an important role in the fabrication of biosensors.

### 2.2.6 Drawbacks

Although MAP has many advantages in microfabrication and has shown great promise for prospective applications, there are still some problems that need to be addressed. Firstly, MAP is generally a serial process, and it is not suitable for mass-production. The structure is fabricated voxel by voxel, and a large complex structure may take hours to fabricate. However, two methods have been proposed to solve this problem. The first approach was reported by Kawata and coworkers<sup>39</sup>. They used a micro-lens array to divide an amplified laser beam into many sub-beams, which were used to fabricate hundreds of structures simultaneously at the same stage. However,

this method requires the distance between individual structures to be close (~ 10 microns) and care needs to be taken to ensure that the laser beam is uniform across micro-lens array.

The second method for addressing the inherently serial nature of MAP is a more general solution. A master structure is fabricated by MAP, and is then molded. Subsequently, the mold is used to make copies. This method has many advantages compared to the micro-lens array technique, but it also has limitations. Although 3D microstructures with closed loops have been fabricated and reproduced using molds<sup>40</sup>, there is a long way to go to make it suitable for industrial mass production of more complex structures.

Secondly, it is difficult to use multi-photon absorption to create free standing 3-D microstructures or components composed of materials such as metals, metal oxides, and this difficulty limits its application in the electronics industry and other fields such as MEMS. Although selective metallization<sup>36, 39</sup> has been proposed a possible solution, more work is necessary to extend MAP to the electronics industry.

Another concern about MAP is 3D pattern or structure deformation resulting from the surface tension of a rinse solution during the developing process. This pattern deformation is not restricted to MAP alone. It is an issue associated with almost all polymeric patterning via lithographic techniques because of the developing process required to isolate polymerized structures. Pattern deformation or collapse is detrimental to precise fabrication, and it is related to the spacing, aspect-ratio and the surface tension of the rinse solution. For example, dense, fine and high aspect-ratio

structures often collapse because they can easily come into contact with each other at their tips.

Park and coworkers<sup>41</sup> have investigated 3D pattern collapse using imperfection finite element model. Figure 4 illustrates how a pattern can be deformed during the developing process. As the rinse solvent evaporates, two adjacent structures can get close enough to each other that they stick to one another at the tip due to the surface tension. Among the methods employed to reduce pattern collapse, surface tension reduction is the most effective because it is independent on the size of the structures. Thus supercritical drying with zero surface tension has been demonstrated as very beneficial in obtaining fine patterns without collapse<sup>42</sup>. However, it is not cheap and it does not give MAP any advantage as an easily accessible technique.

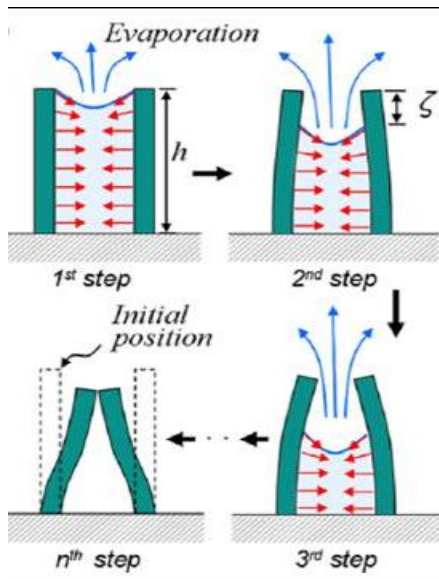


**Figure 4.** Schematic illustration of the mechanism of the pattern distortion due to surface tension of a rinse material<sup>41</sup>

While surface tension might be the main reason for deformation, two other factors should also be considered. One of them is the mechanical properties of the material itself, such as the Young's modulus, a determining factor for the flexibility

and rigidity. The other factor is the interaction between the rinse solvent and the polymeric structure itself such as solvation and swelling. For almost all polymeric patterning techniques, unpolymerized resins are washed away by certain solvents, which may also dissolve or swell the solidified polymeric structures. This factor can effectively reduce the Young's modulus of the polymeric structures and lead to pattern collapse. Our study provides direct proof for this effect.

## Chapter 3: Solvent Study on Towers Fabricated via MAP

### 3.1 Introduction

MAP has showed a strong ability to create arbitrary 3D polymeric microstructures<sup>11,14,18</sup>, which may find use in many micromechanical and microfluidic applications<sup>34,36,38</sup>. With the feature size in polymeric structures fabricated via MAP surpassing 100 nm<sup>27,28,29</sup>, it is becoming increasingly difficult to design and fabricate complex devices with desired characteristics without a deep understanding of the mechanical and the other properties of polymeric structures. Young's modulus, a measure of stiffness, is the key mechanical property for the polymeric materials and structures.

Our group has previously measured the Young's modulus of polymeric micro cantilevers fabricated by MAP and found that it is somewhat smaller (~ a factor of 4) than that of bulk polymers<sup>43</sup>. Other investigators have also measured the elastic properties of polymer nanowires fabricated via MAP, and they reported that the shear modulus is three orders smaller than seen in the bulk polymers<sup>44</sup>. Although both the resins and the dimensions of two structures are different, the magnitude of discrepancy with respect to the decrease in the Young's modulus is astonishing. Our micro cantilevers had a typical width of 10  $\mu\text{m}$  and the diameter of the polymer nanowires is between 150 nm and 1  $\mu\text{m}$ . To bridge this scale gap and get a better understanding of how Young's modulus changes with scale, we fabricated cylindrical towers with diameters ranging from 900 nm to 6 microns and studied how the highest stable aspect ratio obtained changes with diameter. Furthermore, by changing

solvents in the drying process and observing whether towers collapse or not, we found a straightforward way to observe the change in mechanical properties of those towers and to gain insight into how surface tension and other factors may affect the mechanical properties of polymeric structures fabricated via MAP.

### 3.2 Experimental Details

Our resin is prepared by mixing equal parts of ethoxylated (6) trimethylolpropane triacrylate (Sartomer, SR-499) and *tris*(2-hydroxyethyl)isocyanurate triacrylate (Sartomer, SR-368) with 3 wt. % 2,4,6-trimethylbenzoylthoxyphenylphosphine oxide (BASF, Lucirin TPO-L). Both SR-499 and SR-368 have some favorable properties for our study, such as fast curing, heat resistance, hardness, abrasion resistance and low shrinkage. Transparent Lucirin TPO-L has also been demonstrated to be a suitable photoinitiator primarily because of its commercial availability and high miscibility as a liquid. A homogeneous resin is made by mixing the three components for ~ 24 hrs, and then centrifuging the mixture for 30 minutes to remove any bubbles inside the resin. For experiments on different days, the resin is always heated in an oven first and then mixed and centrifuged again to ensure that there is no crystallization in the resin before its use.

The sample is made by sandwiching the resin between a substrate and a cover slip with a spacer in between. The space thickness depends on the maximum height of the structures, and it should not exceed the working distance of the objective used for fabrication. The substrate is usually glass, which is O<sub>2</sub> plasma-cleaned and then immersed in an ethanol solution with 3% by volume of 3-acryloxy-

propyltrimethoxysilane. This reaction creates acrylate groups on the surface of the glass that can then be polymerized into the microstructure, increasing the adhesion between substrate and polymeric structures.

A 800 nm wavelength mode-locked Ti:sapphire laser that delivered 100 fs pulses at a repetition rate of 76 MHz was utilized for MAP. 20X or 40X oil immersion lenses focused the laser into prepolymer resin to fabricate towers with different dimensions. A three-dimensional piezoelectric stage moved the resin relative to the focal spot according to a pre-programmed pattern, and the whole fabrication process was observed through a CCD camera. The stage was controlled by a Labview program written by previous researchers in our lab. This program is able to read txt or excel files that can be written either by hand or by a Labview program. Such files allow the user to set the moving speed of the stage along x,y,z axis, write down coordinate matrix points of our structure, and close or open the shutter.

The laser power used for fabrication was controlled using a half-wave plate and a polarizer. The typical moving speed of stage is 20  $\mu\text{m/s}$  along x,y axis, 2  $\mu\text{m/s}$  along z axis and the power of laser beam is between 5 mW and 40 mW (measured outside objective). The typical distance between two adjacent points in the coordinate matrix was less than the size of focal point to ensure that there is a good overlap. Once fabrication was complete, the unpolymerized resin was washed away by immersing the sample in ethanol twice (with 5 mins for each rinse). The remaining polymerized structure was rinsed in another solvent for 1min before being dried in the air; this solvent is called drying solvent. All fabrication and rinsing was carried out at 20 °C.

## 3.3 Results and Discussions

### 3.3.1 Methods

Three methods were used to fabricate micro towers and one of them was chosen as the best for subsequent fabrication. The first method is fabrication layer-by-layer. Towers with aspect ratio ( $\sim 35$ ) can be made using this method. However, it is generally slow. For example, a tower with a height of over 150  $\mu\text{m}$  takes 20 to 30 mins to fabricate.

The second method was to move the stage straight up along the z-axis (*i.e.*, along the surface normal vector) drawing a straight line. The diameter of such towers (*i.e.*, towers fabricated using this method) is dependent on height of the tower, the power of laser beam, and the scanning speed along the z axis. High laser-beam power and fast fabrication speeds are preferred for this method. It takes less than 30s to fabricate a straight tower with a height of 75 microns. However, only limited heights ( $< 80$  microns) and aspect ratio ( $\sim 25$ ) have been achieved so far. Also the tips of the structures made this way are narrower than the rest part of the tower.

The last fabrication method combined the advantages of the previous two methods described above; it produced structures with high aspect-ratios at a high efficiency. The focal point is moved up along a spiral, and the parameters of the spiral (diameter and spacing between two adjacent layers, etc.) and the laser-beam power are chosen to ensure that there is a good overlap and that the tower has a solid center. A tower with a height of 250  $\mu\text{m}$  and an aspect ratio  $\sim 40$  can be fabricated in 3mins. Moreover, these towers are also more homogeneous and straight. It is possible that fabrication along a spiral reduces the force of flow in x-y plane in layer-by-layer

fabrication. It also avoids the thinner tips in the second method. This method is chosen for the following studies.

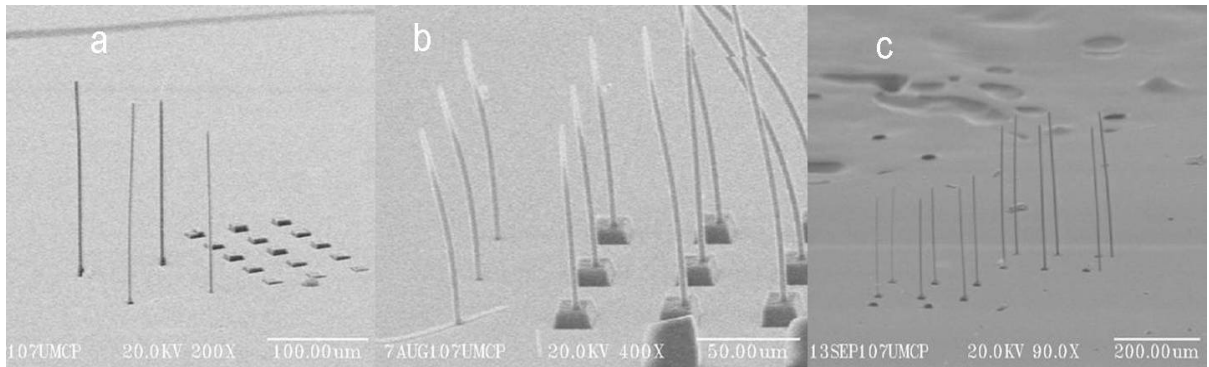


**Figure 5**, Towers fabricated by layer-by-layer(a), going straight up along z-axis(b), going straight along a spiral respectively from left to right(c).

### 3.3.2 Size Study

By changing experimental conditions (laser beam power, scanning speed, parameters for individual spirals etc.), towers with different dimensions can be fabricated. For towers with a certain diameter, there was always a maximum height at which the towers begin bending or collapsing no matter which solvent was used to dry them and this height is called critical height. As shown in Figure 6 (for two different groups of towers dried in different solvents), as the height is increased from right to left, the towers started collapsing at certain height.

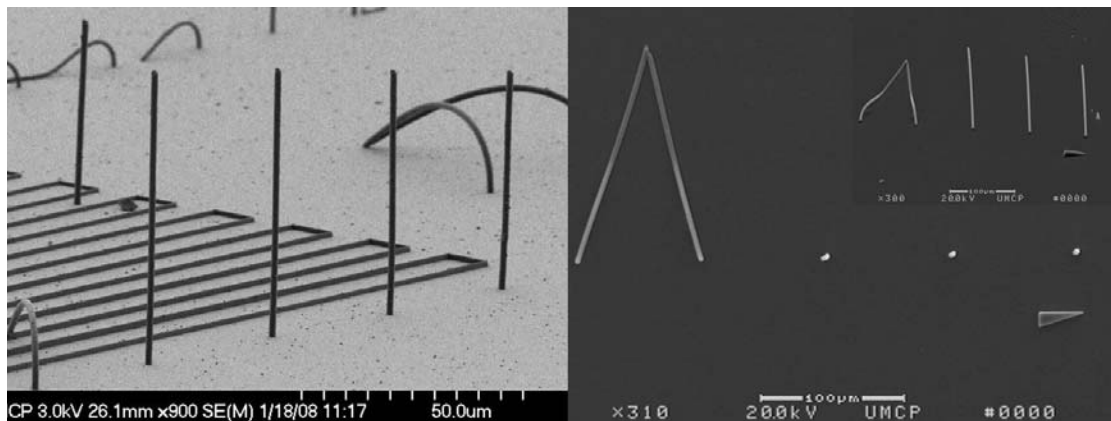


**Figure 6**, Proof of existence of critical height. Left: Objective: 40x oil, power=10mw, dried in n-Hexane, D=1.6 microns, H=50, 55, 60, 65 and 70 microns respectively from right to left. Right: Objective: 20x, power=33 mW, Dried in ethanol, D=3 microns, H=60, 70, 80, 90 and 100 microns respectively from right to left. The inset in the right figure is the side view.

We think that this critical height is determined by the intrinsic mechanical properties of the polymer, in particular the Young's modulus. We found that this critical height was not only dependent on the diameter of the towers, but also dependent on the drying solvent used in the developing process. Firstly, we fabricated towers with different diameters and studied the relationship between critical height and diameter using n-Hexane as the drying solvent. Then we kept the diameters of towers unchanged and studied the influence of the drying solvent on the critical heights. In experiments, a matrix of towers with increasing height was fabricated in a certain order and the critical height was determined from both high resolution SEM measurements and the parameters we set for the size of our towers. It turned out they matched very well. To get a more accurate measurement, the spacing between adjacent towers is often kept large enough to prevent the influence of one tower on another.

Table I shows the critical heights for towers with different diameters dried in n-hexane. Figure 7 is the corresponding height versus diameter (H-D) graph, and it presents a very good linear relationship between the height and the diameter with a slope around 40, which indicates that the critical aspect-ratio is a constant and has a value around 40 for towers with diameters ranging from 900 nm to 6 microns. The reason for this is still unclear, but we know that the Young's modulus does not change a lot as the scale enters submicron level.

D( $\mu\text{m}$ )	Limit H( $\mu\text{m}$ )	Aspect ratio	Fabrication condition
0.90 $\pm$ 0.10	30 $\pm$ 2.5	34 $\pm$ 3	40x 10mw*
1.60 $\pm$ 0.10	67.5 $\pm$ 2.5	42 $\pm$ 2	40x 10mw
3.00 $\pm$ 0.20	115 $\pm$ 10	39 $\pm$ 3	20x 33mw
5.00 $\pm$ 0.20	215 $\pm$ 10	43 $\pm$ 2	20x 33mw
6.00 $\pm$ 0.20	250 $\pm$ 10	42 $\pm$ 2	20x 33mw

**Table 1**, The critical heights for towers with different diameters dried in n-Hexane.  
\*Power is measured outside the objective.

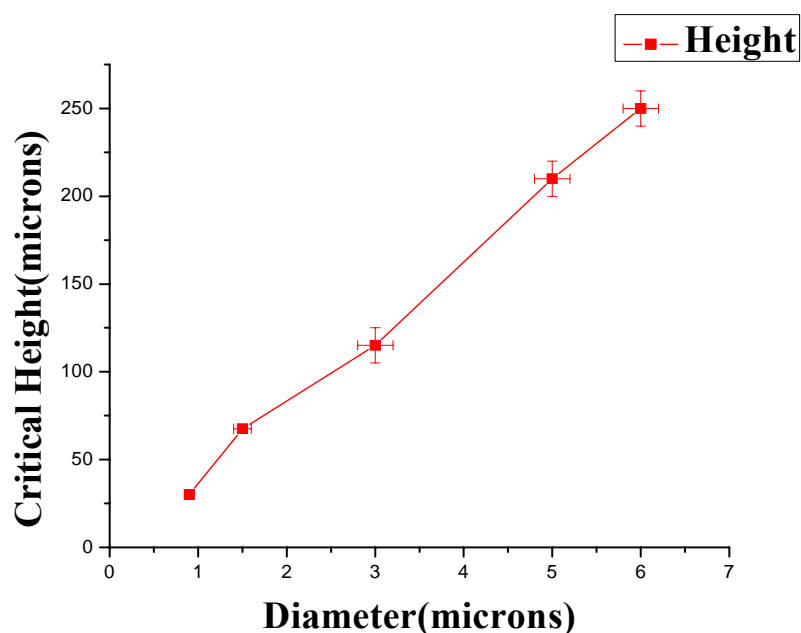


**Figure 7**, H-D graph for towers dried by n-hexane

### 3.3.3 Solvent Study

The drying solvent proved to have a great influence on the critical height and n-hexane appears to be an ideal drying solvent because of its very low surface tension (18.43 mN/m) at 20 °C, easy availability and high evaporation rate which shortens the drying process. As shown in figure 8, compared with n-hexane, ethanol can reduce the critical height significantly by 25 microns and benzene can decrease it further. Since benzene has a surface tension of 28.88mN/m and ethanol has a surface tension

of 22.10 mN/m at 20 °C, it is plausible that larger surface tension leads to lower aspect-ratio.

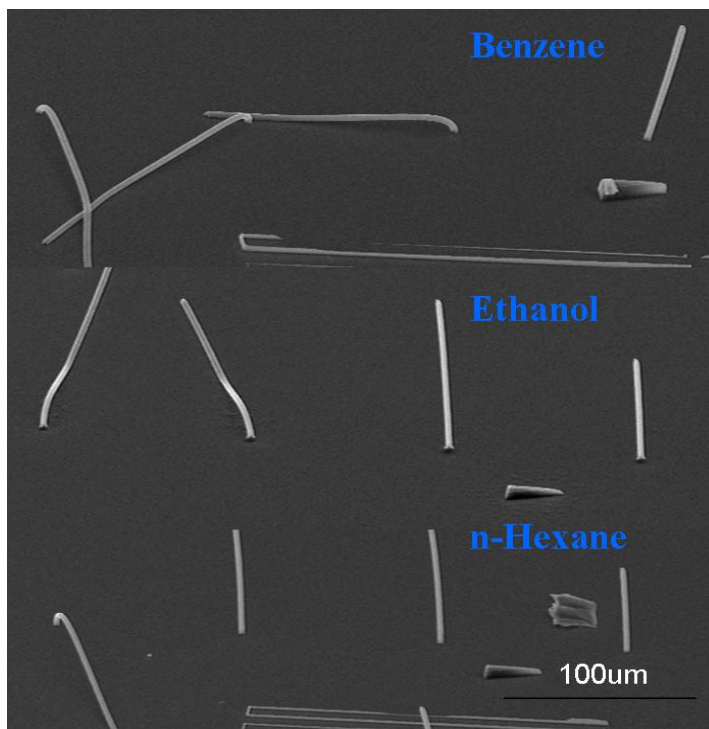


**Figure 8**, Dependence of the critical height on the drying solvent. Objective used: 20x, Laser power=33mw, D=3 microns, H=50, 75, 100 and 125 respectively from right to left. From top to bottom: dried in benzene, ethanol and n-Hexane respectively.

However, without ruling out other possibilities, we cannot conclude that the critical height is dependent on surface tension alone. As we mentioned before, other interactions between the drying solvent and the polymeric structures such as swelling, should not be neglected. Swelling mainly results from similar polarities between polymers and solvent. Here we assume that the polarity of the polymers remains almost the same as that of monomers after polymerization and all polymeric towers have the same polymer density under the same experimental conditions. Then the swelling effect of the drying solvent on polymers can be predicted directly from the ability of the solvent to dissolve monomers. We did a solubility test of SR-368, SR-

499 monomers in benzene, ethanol and n-hexane. We found that benzene and ethanol can dissolve both of them while n-Hexane dissolves neither of them. To examine the effect of swelling on critical height, we chose cyclohexane as the drying solvent for our experiment. Cyclohexane is a solvent with a high surface tension (24.95 mN/m) and a fast evaporation rate. It dissolves neither of monomers mentioned above. A decrease of 10 microns in critical height is observed and it is less than that of ethanol which even has lower surface tension (22.10 mN/m). Thus we can conclude that both surface tension and swelling play an important role in reducing critical aspect-ratio.

We also used n-decane which has a surface tension of 23.83 mN/m, between the value of n-hexane and cyclohexane and it can dissolve neither SR-368 nor SR-499. It turned out n-decane reduced critical height by 25 and this value is larger than that of cyclohexane which has larger surface tension. However, because n-decane has a very slow evaporation rate, it is entirely possible that the residual liquid of n-decane on the tower cannot go away very quickly and exerts a downward stress on the tower. We tried to find another solvent that cannot dissolve either of the monomers, that has a surface tension constant between n-hexane and cyclohexane, and has a high evaporation rate, but we were unsuccessful.

### 3.3.4 Applications

Our findings provide great insight into how to choose appropriate drying solvents to get better aspect ratios for the structures fabricated via MAP. Generally, a solvent with low surface tension and high evaporation rate as well as a low solubility of monomers is preferred. The strong towers (see picture 5 and 6 in Figure 9) fabricated have possible applications as micro cantilevers or microelectrodes. Our strategy of

studying mechanical properties of one certain material can also be expanded to other materials, providing a simple method to evaluate their mechanical properties on microscale without measuring their true Young's modulus. Furthermore, our method of fabrication of towers can be applied to other materials that could be used for MAP, and it can also directly be applied to fabricate standing homogeneous pipes by increasing the diameter of a spiral (see 1-4 in figure 9). Those pipes can be fabricated in a very short time and they are very strong and they have smooth surfaces. They can be used as miniaturized container or micro reactor with volume on nanoliter scale in microfluidics. For example, figure 9-4 shows a pipe with a diameter of 8 microns and a height of 20 microns and the wall thickness for this pipe is around 600 nm.

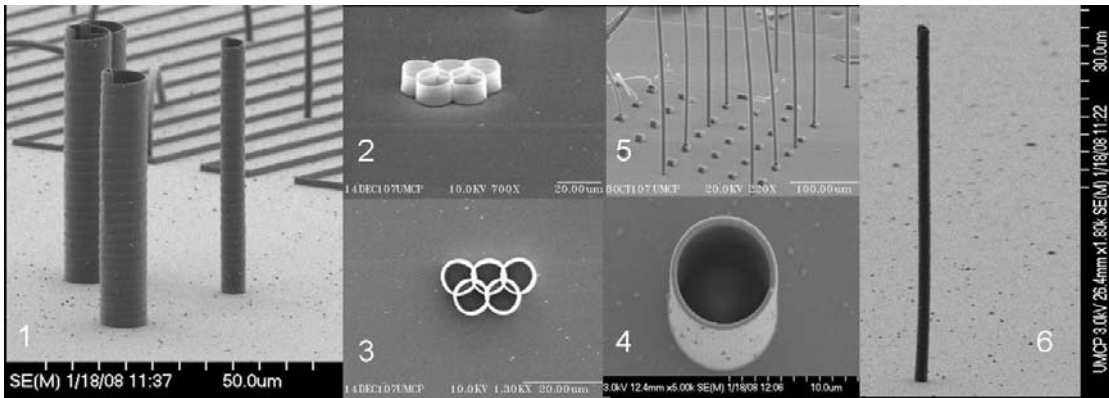


**Figure 9**, Pipes and towers fabricated via MAP using our method.

### 3.4 Summary

We found a fast method to fabricate high-aspect-ratio polymeric micro towers using a multi-photon absorption polymerization technique and studied the best aspect-ratio of towers at different conditions by varying laser-scanning parameters and laser-beam power. The best aspect ratio is a constant ( $\sim 40$ ) and it is independent on the size

of towers with diameters ranging from 900 nm to 6 microns. We proved that the aspect ratio does not decrease a lot as the size of tower goes into sub-micron level and we also proved that surface tension is not the only factor that leads to lower aspect ratios.

## Chapter 4: Conclusion

This thesis has briefly reviewed conventional micro patterning techniques and described Multiphoton Absorption Polymerization (MAP) in details in the second chapter. As a unique method with the strong ability to fabricate arbitrary 3-D microstructures, MAP is used to fabricate micro towers and pipes with different sizes in chapter 3. We found a method to fabricate towers efficiently and studied the relationship between the best aspect ratio and the diameter of towers. We found that the best aspect-ratio is a constant ( $\sim 40$ ) and it is independent on the size of towers with diameters ranging from 900 nm to 6 microns. We also directly proved that surface tension is not the only factor causing pattern collapse. To get structures with best aspect ratio in MAP, surface tension and swelling as well as the evaporation rate of the drying solvent should all be considered. Towers and pipes with good aspect ratio and smooth surfaces were fabricated in a short time and they may have direct applications in the future.

## References

- [1] Reyes, D. R. ; Iossifidis, D.; Auroux, P.-A.; Manz, A. *Analytical Chemistry* **2002**, 74,2623.
- [2] Peeni, B.A.; Lee, M.L.; Hawkins, A.R. *Electrophoresis* **2006**, 27(24), 4888-4895
- [3] Malek, C.; Saile, V.; *Microelectron. J.* **2004**, 35, 131.
- [4] Xia, Y. *Angew Chem, Int Ed* **1998**, 37, 550
- [5] Bertsch, A.; Lorenz, H.; Renaud, P. *Sensors and Actuators, A: Physical* **1999**, A73,14.
- [6] Maruo, S.; Ikuta, K. *Sensors and Actuators, A: Physica* **2002**, A100, 70.
- [7] Göppert-Mayer M. "Über Elementarakte mit zwei Quantensprüngen". *Ann Phys* **1931**, 9: 273–95
- [8] Blanca, C.M.; Hell, S. *Opt. Express* **2002**, 893.
- [9] LaFratta, C.N. Ph.D thesis **2006**. Multiphoton absorption polymerization; issues and solutions.
- [10] Pitts, J.D.; Campagnola, P.J.; Epling, G.A.; Goodman, S.L. *Macromolecules* **2000**, 33(5), 1514-1523.
- [11] Cumpston, B.H.; Ananthavel, S.P.; Barlow, S.; Dyer, D.L.; Ehrlich, J.E.; Erskine, L.L.; Heikal, A.A.; Kuebler, S.M.; Lee, I.Y. Sandy; McCord-Maughon, D.; Qin, J.; Rockel, H.; Rumi, M.; Wu, X.; Marder, S.R.; Perry, J.W. *Nature (London)* **1999**, 398(6722), 51-54 .
- [12] Maruo, S.; Nakamura, O.; Kawata, S. *Optics Letters* **1997**, 22, 132.
- [13] Sun, H.-B.; Tanaka, T.; Takada, K.; Kawata, S. *Applied Physics Letters* **2001**, 79, 1411.
- [14] Kawata, S.; Sun, H. B.; Tanaka, K. ; Takada, K. *Nature* **2001**, 412, 697.
- [15] Serbin, J.J.; Chichkov, B.N. *Proceedings of SPIE-The International Society for Optical Engineering* **2003**, 5118
- [16] Bhuian, B.; Winfield, R. J.; O'Brien, S.; Crean, G. M. *Applied Surface Science* **2006**, 252(13)
- [17] Teh, W. H. ; Durig, U. ; Salis, G.; Harbers, R.; Drechsler, U.; Mahrt, R. F.; Smith, C. G.; Guntherodt, H. J.; *Applied Physics Letters* **2004**, 84, 4095.
- [18] W. H. Teh, U. Duerig, U. Drechsler, C. G. Smith, H. J. Guentherodt, *Journal of Applied Physics* **2005**, 97, 054907/1.
- [19] Reinhardt, B.A.; Brott, L.L.; Clarson, S.J.; Dillard, A.G.; Bhatt, J.C.; Kannan, R.; Yuan, L.; He, G. S.; Prasad, P.N. ; *Chemistry of Materials* **1998**, 10(7)
- [20] Adronov, A.; Frechet, Jean M. J.; He, G.S.; Kim, K.-S.; Chung, S.-J.; Swiatkiewicz, J.; Prasad, P. N. *Chemistry of Materials* **2000**, 12(10), 2838-2841.
- [21] Kannan, R.; He, G.S.; Yuan, L.; Xu, F.; Prasad, P.N.; Dombroskie, A.G.; Reinhardt, B.A.; Baur, J.W.; Vaia, R.A.; Tan, L.-S. *Chemistry of Materials* **2001**, 13 (5).
- [22] Rumi, M.; Ehrlich, J.E.; Heikal, A.A.; Perry, J.W.; Barlow, S.; Hu, Z.; McCord-Maughon, D.; Parker, T.C.; Roeckel, H.; Thayumanavan, .; Marder, S.R.; Beljonne, D.; Bredas, J.-L. *Journal of the American Chemical Society* **2000**, 122(39), 9500-9510
- [23] Albota, M; Beljonne, D; Bredas, J L; Ehrlich, J E; Fu, J Y; Heikal, A A; Hess, S E; Kogej, T; Levin, M D; Marder, S R; McCord-Maughon, D; Perry, J W; Rockel H;

- Rumi, M; Subramaniam, G; Webb, W W; Wu, X L; Xu C *Science* (New York, N.Y.) **1998**, 281(5383)
- [24] Belfield, K.D.; Ren, X.; Van S, Eric W.; Hagan, D.J.; Dubikovsky, V.; Miesak, E.J. *Journal of the American Chemical Society* 2000, 122(6), 1217-1218
- [25] Kuebler, S.M.; Braun, K.L.; Zhou, W.H.; Cammack, J.K.; Yu, T.Y.; Ober, C.K.; Marder, S.R.; Perry, J.W. *J. Photochem. Photobiol.* **2003** A 158, 163
- [26] Sun, H.-B.; Tanaka, T.; Kawata, S. *Applied Physics Letters* 2002,80(20).
- [27] Takada, K.; Sun, H.-B.; Kawata, S. *Applied Physics Letters* **2005**, 86(7);
- [28] Haske, W.; Chen, V.W.; Hales, J.M.; Dong, W.; Barlow, S.; Marder, S.R.; Perry, J.W. *Optics Express* **2007**, 15(6), 3426-3436 .
- [29] Tan, D.; Li, Y.; Qi, F.; Yang, H.; Gong, Q.; Dong, X.; Duan, X.. *Applied Physics Letters* **2007**, 90(7),
- [30] Lee, W.; Pruzinsky, S.A.; Braun, P.V. *Advanced Materials* (Weinheim, Germany) **2002**, 14(4), 271-274
- [31] Serbin, J.; Ovsianikov, A.; Chichkov, B. *Optics Express* **2004**, 12(21), 5221-5228
- [32] Klein, S.; Barsella, A.; Leblond, H.; Bulou, H.; Fort, A.; Andraud, C.I.; Lemercier, G.; Mulatier, J. C.; Dorkenoo, K. *Applied Physics Letters* **2005**, 86(21)
- [33] Passinger, S.; Proceedings of SPIE-The International Society for Optical Engineering 2006, 6195
- [34] Galajda, P.; Ormos, P. *Applied Physics Letter.* **2001**,78,249-251.
- [35] Kuebler, S. M.; Rumi, M.; Watanabe, T. ; Braun, K.; Cumpston, B. H.; Heikal, A. A.; Erskine, L. L.; Thayumanavan, S.; Barlow, S. ; Marder, S. R.; Perry, J. W. *J. Photopolym. Sci. Technol.* **2001**, 14, 657-668.
- [36] Farrer, R.A.; LaFratta, C.N.; Li, L.; Praino, J.; Naughton, M.J.; Saleh, B.E. A.; Teich, M.C.; Fourkas, J.T. *Journal of the American Chemical Society* 2006, 128(6)
- [37] Basu, S.; Cunningham, L.P.; Pins, G.D.; Bush, K.A; Taboada, R.; Howell, A.R.; Wang, J.; Campagnola, P.J. *Biomacromolecules* **2005**, 6(3), 1465-74
- [38] Zhou, W. ; Kuebler, S. M. ; Braun, K. L. ; Yu, T. ; Cammack, J. K. ; Ober, C. K. ; Perry, J. W. ; Marder, S. R. *Science* **2002**,296,1106-1109
- [39] Formanek,F.; Takeyasu,N.; Tanaka,T.; Chiyoda,K.; Ishikawa, A.; Kawata,S. *Optical Express* **2006**,14(2),800-809
- [40] LaFratta, C.N.; Li, L.; Fourkas, J.T. *Proc. Nat. Acad. Sci.* **2006**,103, 8589-8594
- [41] Park, S.H.; Kim, K.H.; Lim, T.W.; Yang, D.Y.; Lee, K.S.; *Microelectronic Engineering* **2008**, 85(2), 432-439
- [42] Hideo,N., Kenji,Y.; Kenji,K. *Microelectronic Engineering* **1999**, 46(1), 129-132
- [43] Baldacchini,T; LaFratta,C.N.; Farrer,R.A.; Teich,M.C.; Saleh, Bahaa E. A.; Naughton,M.J.; Fourkas, J.T. *Journal of Applied Physics.* **2004**, 95, 6072
- [44] Nakanishi,S.; Shoji,S.; Kawata,S.; Sun,H.-B. *Journal of Applied Physics.***2007**, 91, 063112